Supplementary

On the Spectral Identification and Wavelength Dependence of Rare-Earth Ore Emission by Laser-Induced Breakdown Spectroscopy

Muhammad Sher Afgan, Zongyu Hou, Weiran Song, Jiachen Liu, Yuzhou Song, Weilun Gu and Zhe Wang *

State Key Laboratory of Power Systems, International Joint Laboratory on Low Carbon Clean Energy Innovation, Department of Energy and Power Engineering, Tsinghua University, Beijing 100084, China
* Correspondence: zhewang@tsinghua.edu.cn

Citation: Afgan, M.S.; Hou, Z.; Song, W.; Liu, J.; Song, Y.; Gu, W.; Wang, Z. On the Spectral Identification and Wavelength Dependence of Rare-Earth Ore Emission by Laser-Induced Breakdown Spectroscopy. *Chemosensors* **2022**, *10*, 350. https://doi.org/10.3390/chemosensors10090350

Academic Editor: José M. Amigo

Received: 11 July 2022
Accepted: 23 August 2022
Published: 25 August 2022

Supplementary Figure S1 shows emission spectra from 250–433 nm from the echelle spectrograph. The spectra mostly consisted of noise in the spectral range of 190–250 nm at the delay time of 3 μs. Hence, they were not shown.

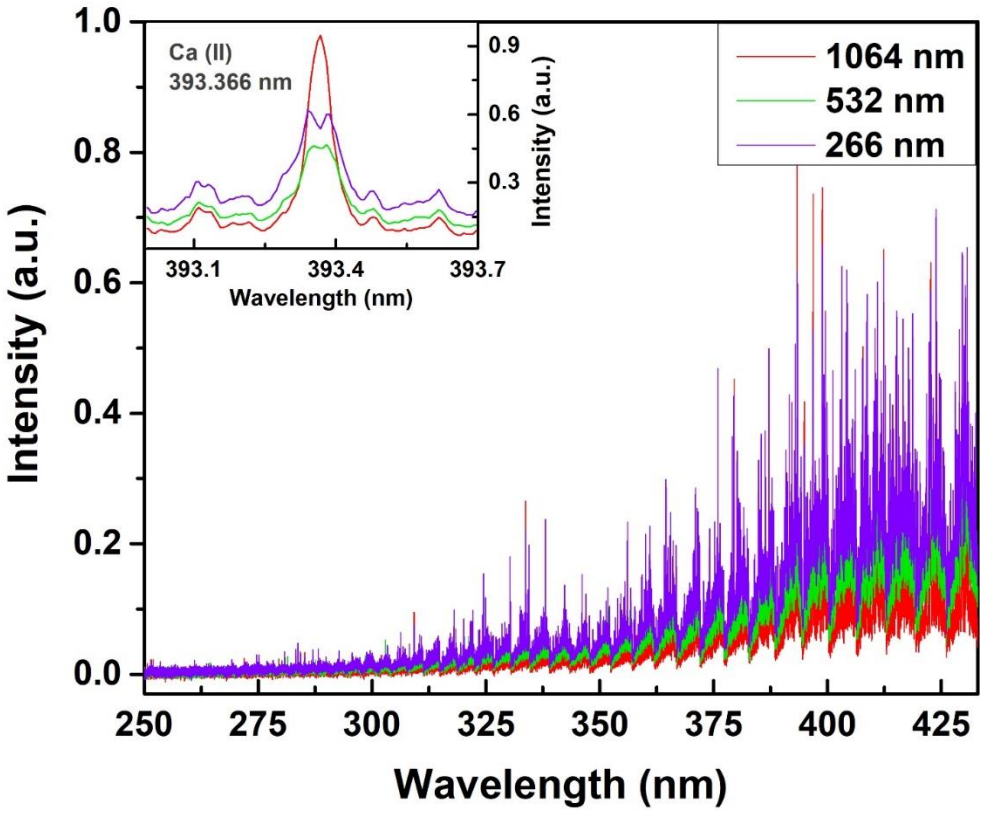

Figure S1. The monazite ore spectra with 1064 nm, 532 nm and 266 nm laser wavelengths at the same laser fluence in the spectral range of 250–433 nm of the echelle spectrograph. The inset shows a major element emission line Ca (II) 393.366 nm. The higher intensity with 1064 nm shows higher temperature, while self-reversal with 266 nm indicates stronger ablation conditions, as described in the manuscript.

Supplementary Figure S2 shows the entire spectral range of 190–930 nm captured by the Czerny–Turner spectrometer at a 3 μs delay. The spectral trend in Figure S1 and S2 is the same, except for the laser line appearance at 266 nm in the time integration spectrometer. The self-reversal of the 393.366 nm line for 532 and 266 nm is also completely masked in Figure S2 due to the limited spectrometer resolution. In addition, the intensity of the

molecular bands consistently increased (especially visible above 550 nm) with the lowering of the laser wavelength due to enhanced material ablation, as described in the manuscript.

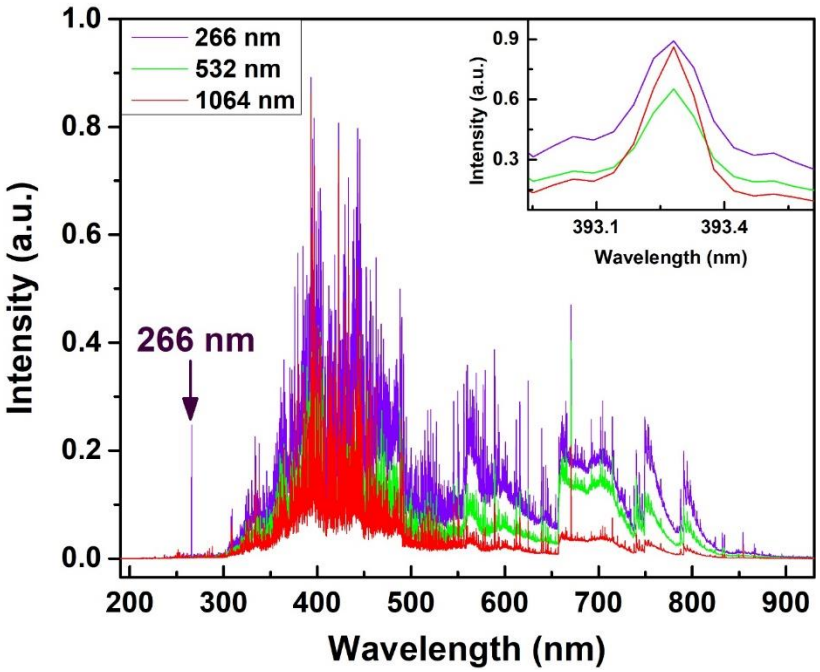

Figure S2. The monazite ore spectra with 1064 nm, 532 nm and 266 nm laser wavelengths at the same laser fluence in the spectral range 190–930 nm of the Czerny–Turner spectrometer. The inset shows Ca (II) 393.366 nm and the self-reversals are masked due to the limited spectrometer resolution. The laser line was also observed at 266 nm, which is marked in the figure.

Supplementary Figure S3 shows the change in emission intensities with variation in electron number density at a fixed temperature. As seen from the Figure, the relative position of the lines did not change while overall intensity is enhanced with increasing electron number density.

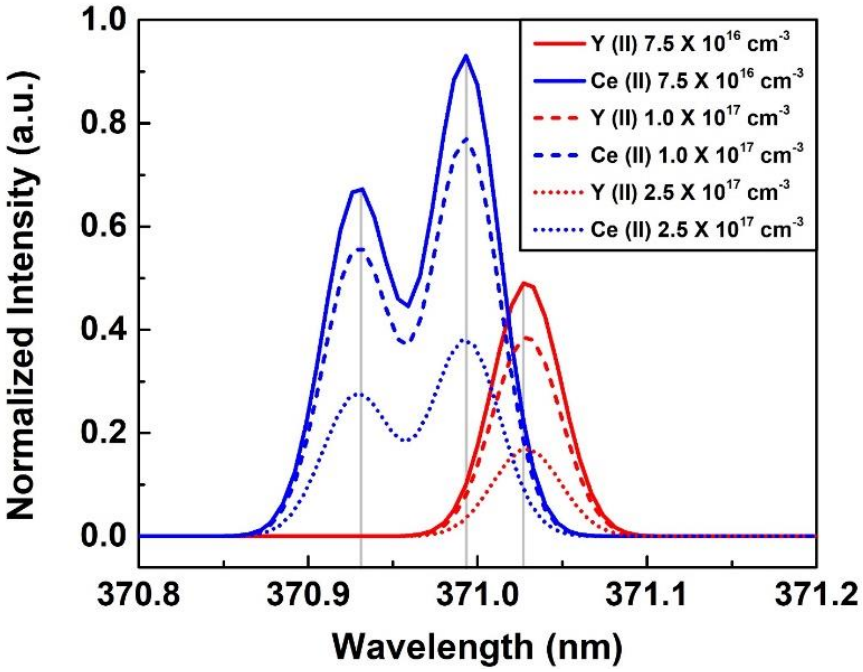

Figure S3. Change in emission intensity at constant temperature conditions (T = 6000 K) and different electron number density (n_e) conditions.

Supplementary Figure S4 shows a Boltzmann plot of the Nd (II) lines. The spectroscopic data of these lines are given in Table S2.

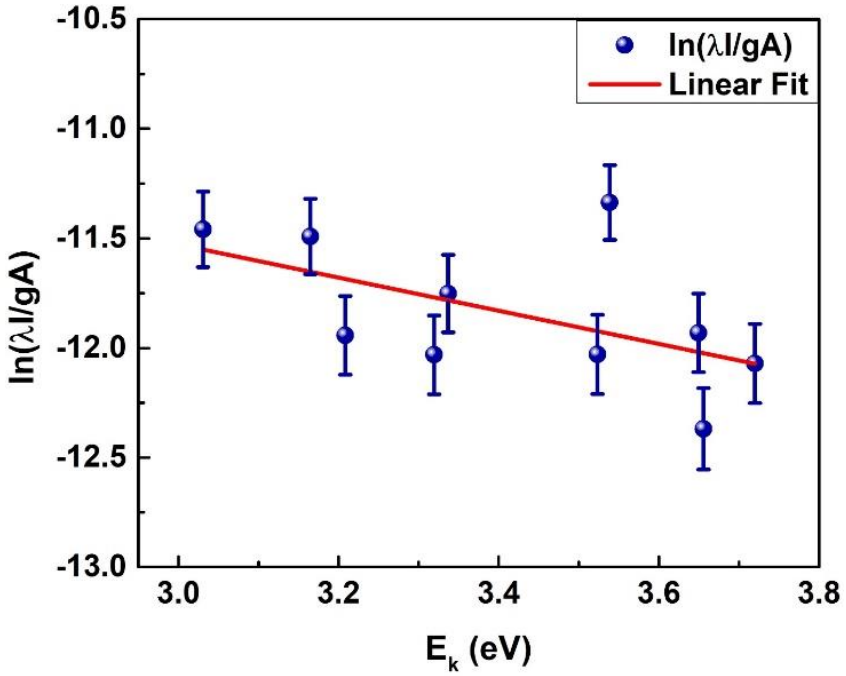

Figure S4. The Boltzmann plot of twelve Nd (II) lines used to calculate the temperature. On the *x*-axis, E_k is the upper energy level in eV. On the *y*-axis, λ is wavelength, I is intensity, g is the statistical weight of the upper level and A is the transition pobability.

Supplementary Figure S5 shows a Lorentz fit for the electron number density measurement.

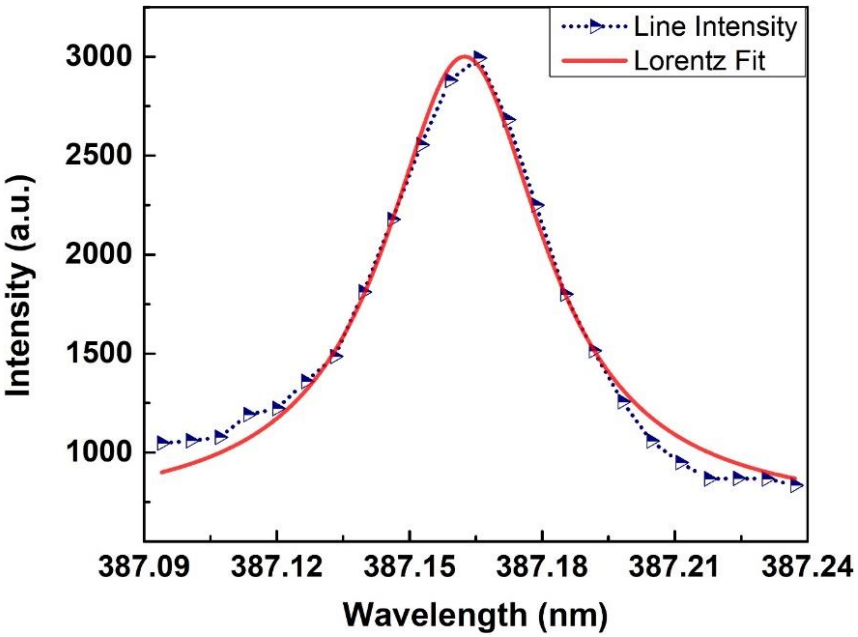

Figure S5. The Lorentz Fit of La (II) 387.166 nm line for electron number density calculation. The delay time for the line shown was a 2.5 μs delay and the electron number density was 1.0×10^{7} cm^{-3}.

Supplementary Table S1 shows the elements and their concentration used for simulated REE spectra. Supplementary Table S2 shows the spectroscopic data used to measure temperature by Nd (II) emission lines.

Table S1. The relative concentration of elements (total 100%) used to obtain the simulated spectra of REE ore.

Element	Percentage (%)
Cerium (Ce)	23.41
Lanthanum (La)	11.22
Neodymium (Nd)	10.05
Praseodymium (Pr)	2.48
Samarium (Sm)	1.35
Yttrium (Y)	0.39
Oxygen (O)	15
Calcium (Ca)	15
Silicon (Si)	16.5
Thorium (Th)	4.6

Table S2. The spectroscopic data of the Nd (II) lines used to measure temperature.

Wavelength	Upper level energy	Lower level energy	Statistical weight		Transition probability
Nd (II) (nm)	E_k (eV)	E_i (eV)	g_k (Upper)	g_i (Lower)	A (s^{-1})
378.425	3.65563	0.38023	12	12	5.5×10^7
385.166	3.53863	0.32056	16	14	9.1×10^6
390.021	3.64938	0.47138	14	16	3.95×10^7
394.151	3.20836	0.06364	10	10	4.13×10^7
395.115	3.31931	0.18227	12	12	3.93×10^7
401.225	3.71981	0.63054	20	18	1.34×10^8
406.108	3.5235	0.47138	18	16	8.0×10^7
410.945	3.33676	0.32056	16	14	5.5×10^7
415.608	3.16463	0.18227	14	12	4.02×10^7
417.732	3.03084	0.06364	12	10	2.52×10^7